Structural Analogy Between β′ Triacylglycerols and *n*-Alkanes. Toward the Crystal Structure of β′-2 p.p+2.p Triacylglycerols

Jacco van de Streek*[a,b], Paul Verwer[a], René de Gelder[c], and Frank Hollander[b]

[a]CAOS/CAMM Center, [b]Department of Solid State Chemistry, and [c]Crystallography Laboratory, University of Nijmegen, Nijmegen, The Netherlands

ABSTRACT: The structural elements of the β′-2 polymorph of 1,3-dilauroyl-2-myristoylglycerol as found by Birker *et al.* (*J. Am. Oil Chem. Soc. 68*:895–906,1991) were also observed in the crystal structures of other long-chain compounds. This analogy led to the assembly of a β′-2 structure at the atomic level from known crystallographic data. The structure was optimized by molecular mechanics and was consistent with experimental data, including satisfactory reproduction of the X-ray powder pattern. To the best of our knowledge, this is the first β′ structure with a 1,2 configuration and an intramolecular orthorhombic subcell which is fully optimized by molecular mechanics to date. It shows all structural elements found earlier by Birker *et al.*

Paper no. J9091 in *JAOCS 76,* 1333–1341 (November 1999).

KEY WORDS: β′, crystal structure, fat, molecular modeling, powder diffraction, triacylglycerol.

Triacylglycerols (TAG) are esters of glycerol with three fatty acids. In the style of De Jong (1), we will denote a TAG by p.q.r where p, q, and r are the lengths of its three fatty acids, e.g., 12.14.12 for 1,3-dilauroyl-2-myristoylglycerol. TAG are important ingredients in many foods. In some foods such as margarines, where they are present in crystalline form, the particular polymorph determines the overall physical properties. Many polymorphs are known, and the stable ones are roughly classified as β and β′ according to their X-ray powder diagrams. Several structural features are recognized for these TAG polymorphs. The molecular configuration (Fig. 1) will have a direct effect on the conformation of the glycerol moiety. The arrangement of two TAG (Fig. 2), in combination with the tilt of the alkane chains with respect to the plane through the methyl end groups, determines the long-spacing reflections in the powder diagram. The subcell of the acyl chains (Fig. 3) is expected to be responsible for the characteristic short-spacing reflections in the powder diagrams: one at 4.6 Å for β, and two or more around 3.8 and 4.2 Å for β′. For pure compounds, p, q, r, their parity, and the presence of any double bonds determine which polymorph has the lowest free energy. Only the structure of the most stable polymorph of p = q = r or p.p.p (p even, saturated) is known in detail (2–5). This is a β-2 modification. For TAG of the type p.p+2.p (p even, saturated), for which β′ is the most stable polymorph, only rough structural information is known. In 1991, Birker *et al.* (6) published a variety of structural elements of the β′-2 structure of 12.14.12, but a final structure at the atomic level could not be obtained. A summary of their findings will be given here.

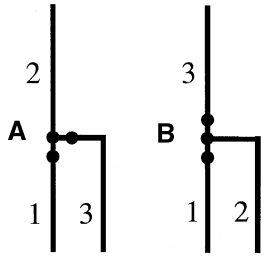

FIG. 1. Configuration of a triacylglycerol (TAG). Two of the three alkane chains are adjacent. If p = r, chains 1 and 3 are indistinguishable and there are two options, either the 1,3 configuration (A) or the 1,2 (= 3,2) configuration (B).

From the long-spacing reflections, it was clear that the TAG molecules formed a β′-2 arrangement. The unit cell parameters for 12.14.12 were determined to be a = 22.9 Å, b = 5.7 Å, c = 66.8 Å, α = 90°, β = 91°, γ = 90°, Z = 8, ρ = 1.016 g/cm^3. This implied that there were four acyl chains along the **c**-axis. Systematic absences pointed to the orthorhombic space groups *Ic*2*a* or *Im*2*a*, but since β ≠ 90°, only the monoclinic subgroups *I*2 or *Im* were possible. It was stressed that

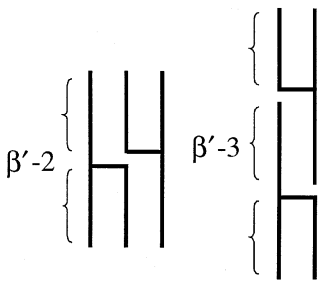

FIG. 2. Arrangement of two TAG. The two possibilities give rise to a β′-2 and a β′-3 polymorph. See Figure 1 for abbreviation.

*To whom correspondence should be addressed at CAOS/CAMM Center, University of Nijmegen, Toernooiveld 1, 6525 ED Nijmegen, The Netherlands. E-mail: hugom@sci.kun.nl

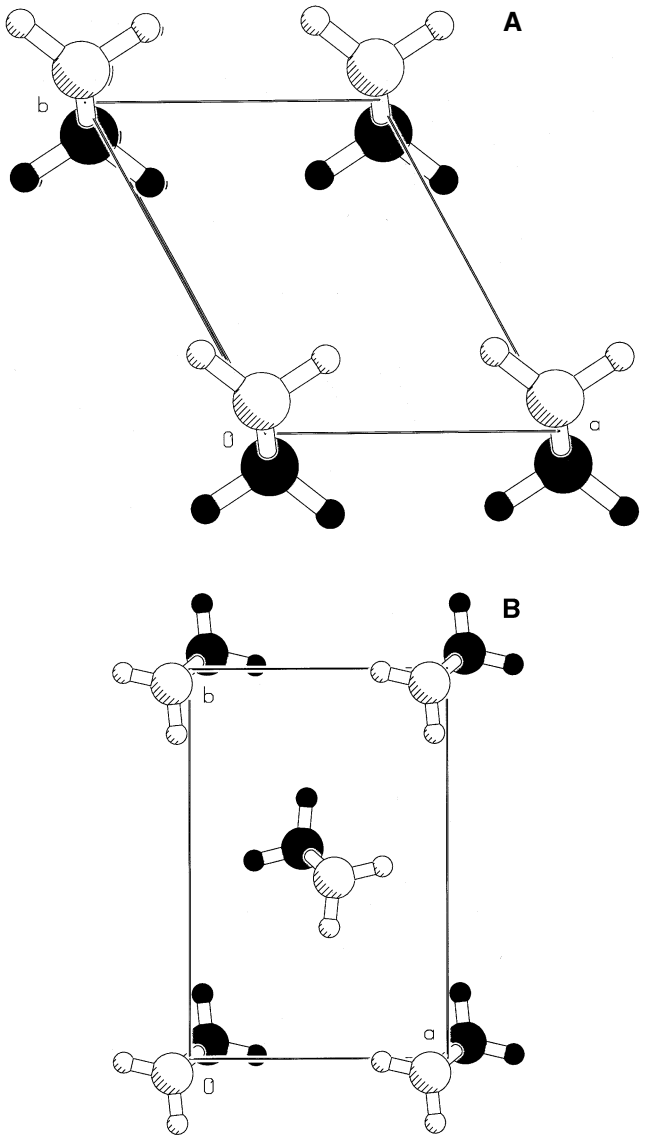

FIG. 3. (A) Triclinic ($T_{//}$) subcell, characteristic for β modifications. a = 4.33 Å, b = 5.46 Å, c = 2.54 Å, α = 72.7°, β = 109.3°, γ = 121.6°. (B) Orthorhombic ($O_{\perp}$) subcell, characteristic for β′ modifications. a = 7.40 Å, b = 4.95 Å, c = 2.54 Å, α = β = γ = 90°. Shaded atoms lie c/4 above the plane of the paper; solid atoms lie c/4 below the plane of the paper. Molecular drawings were prepared using PLUTON (Ref. 27).

the symmetry of the overall structure was very close to orthorhombic. *Im* was rejected because of the improbability of the presence of a mirror plane through a TAG molecule. Diffraction measurements were carried out on a series of p.p+2.p compounds and the increase of c going from 10.12.10 to 16.18.16 was 27.7 Å. It was assumed, based on the linear increase in melting point, that the compounds form a homologously isomorphous series. Since each $-C_2H_4-$ unit has a length of 2.54 Å, and $3 \times 4 \times 2.54$ Å = 30.5 Å, a tilt angle of 65° could be inferred for the alkane chains. An orthorhombic ($O_{\perp}$) subcell could be placed in the **ab** plane if the subcell was tilted approximately 63° in the **bc** plane, which was in agreement with the tilt derived for the chains. The presence of a true $O_{\perp}$ subcell was rejected, with the argument being that this would weaken $h = 3n$ reflections. We disagree on this point, as will be discussed later on. The combination of tilt angle, number of molecules along **c**, the $O_{\perp}$ subcell, and space-group symmetry forced the molecules to be bent at the glycerol moiety. The comparison of binary mixtures of TAG of different chain lengths led to the conclusion that the molecules of the p.p+2.p β′ adopted a 1,2 configuration. These results led Birker *et al*. to the rough structure depicted in Figure 4.

Earlier this year the observation was made (7) that all cell parameters other than c remained constant throughout the p.p+2.p series, a point on which Birker *et al*. (6) did not comment in their paper. Van Langevelde *et al.* (7) showed that if the 10.12.10 molecule is not bent at the glycerol moiety, it cannot be tilted, confirming the findings by Birker *et al.*

The objective of this paper is to propose a structure at the atomic level for p.p+2.p β′-2, which is in agreement with experimental data, which shows the features found by Birker *et al*., and which can be optimized by molecular mechanics. Assuming that the acyl chains, through their size and number, contribute significantly to the structural features of TAG, a logical step would be to look for structural analogs among the *n*-alkanes (unbranched, saturated hydrocarbons which we will denote by the length of their chains, e.g., C28 stands for n-$C_{28}H_{58}$). Two structures following exactly the pattern outlined above for the β′-2 p.p+2.p series were published (8). They show that C28 and C36 are homologously isomorphous and have identical unit cells (apart from c) which are related to the unit cells of β′-2 p.p+2.p, as indicated in Figure 4 and Table 1. The chains are tilted by 63° and form an $O_{\perp}$ subcell. These analogies with the β′ structure suggest that the crystal structures of C28 and β′-2 p.p+2.p are strongly related and that information on the latter can be extracted from other alkane chain-containing crystal structures that have been studied at the atomic level. Especially helpful is the crystal

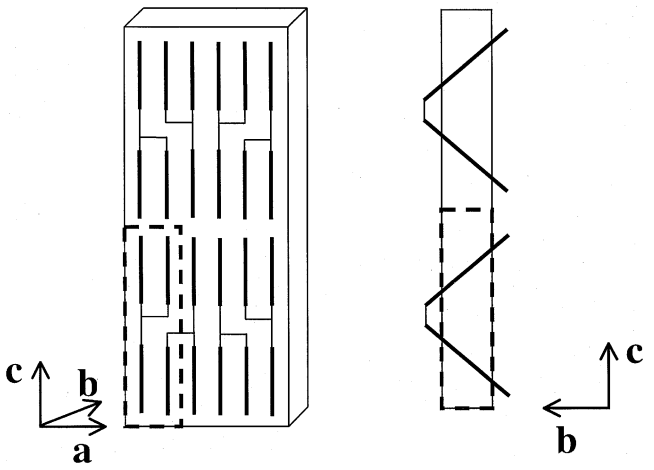

FIG. 4. Rough structure for β′-2 12.14.12 as proposed by Birker *et al.* (6). Bold lines represent acyl chains, connected by glycerol groups. The dashed lines indicate the relation to the C28 crystal structure.

TABLE 1
Relation Between the Experimental Unit Cells of C28/C36 and β′-2 p.p+2.p

C28/C36	p.p+2.p
$3a$ = 22.26 Å	a = 22.9 Å
b = 5.59 Å	b = 5.7 Å
Δc(C36 − C28) = 18.00 Å	Δc(16.18.16 − 12.14.12) = 18.7 Å
α = β = γ = 90°	α = γ = 90°, β = 91°

structure of 16.16.2 (9), the only structure elucidated where the TAG adopt a 1,2 configuration.

Using the currently available Cerius^2 (10) visualization and molecular modeling software, we have been able to assemble a hypothetical β′ structure for 10.12.10 utilizing already known structural elements. This structure, a template for the p.p+2.p series (p even), is in full agreement with the rough structure proposed by Birker *et al*. and shows similarities with the *n*-alkanes. It is stable upon optimization by molecular mechanics and is in agreement with powder diffraction data.

METHODS

Chain packing and molecular conformation. Focusing on the alkane-chain packing, the Cambridge Structural Database (CSD) (11) was searched for all *n*-alkane crystal structures in which the tilt, subcell, and unit cell are commensurate with those of the p.p+2.p β′-2 crystal structure proposed by Birker *et al*. In all known polymorphs from C6 to C36, *n*-alkane chains crystallize in an extended all-*trans* conformation with neighboring chains parallel within layers. All conditions on tilt, subcell, and unit cell were met by a polymorph of C28. In a paper by Boistelle *et al.* (8) on this compound, the homologously isomorphous structure of C36 is described as well. In Figure 4 and Table 1, the experimental cell parameters for p.p+2.p and C28/C36 are compared. The extra oxygens incorporated in the β′ unit cell account for the slightly larger *a* and *b* parameters. The absolute values of *c* are incomparable due to the presence of the glycerol groups in the p.p+2.p unit cells. However, the increments in *c* going from one member of a series to the next (Δc) can be compared and were expected to be exactly the same. It turned out, however, that Δc was slightly larger for the p.p+2.p series as well. This can be explained by assuming that the ideal tilt angle as found in *n*-alkanes is slightly distorted in TAG by the presence of the glycerol moiety. This implies that the angle of tilt would approach the ideal angle on the elongation of the chains leading to smaller Δc units along the series, as was found by Van Langevelde *et al.* (7).

A problem that is not addressed by considering only *n*-alkane structures is the conformation of the glycerol group of the 10.12.10 molecule. In 1991, when Birker *et al*. published their paper, all TAG crystal structures solved were of the β-2 p.p.p type, in which the molecules adopt a 1,3 configuration. Birker *et al.* did not mention the examples of 1,2 configurations present in diacylglycerols, namely in the homologously isomorphous structures of 12.12.0 (12) and 16.16.0 (13). Even though the two acyl chains within one molecule form an $O_\perp$ subcell, as required by the β′ structure, we will not use these structures based on the assumption that the presence of the hydrogen bonding scheme and the lack of steric hindrance will affect the conformation of the glycerol group too much. Several substituted diacylglycerols, all in the 1,2 configuration but not mentioned by Birker *et al.* either, were known as well: sodium 1,2-dilauroyl-*sn*-phosphatidate (14), 1,2-dilauroyl-*rac*-phosphatidylethanolamine (15), 1,2-dilauroyl-*rac*-phosphatidyl-*N*,*N*-dimethylethanolamine (16), and 1,2-dimyristoyl-*sn*-phosphatidyl-*N*,*N*,*N*-trimethylethanolamine (17; no coordinates are given). Even though 1,2-dilauroyl-*rac*-phosphatidyl-*N*,*N*-dimethylethanolamine (16) has an intramolecular $O_\perp$ subcell, we will not use these structures assuming that the presence of the zwitterionic group will affect the conformation of the glycerol group too much.

The first example of a 1,2 configuration in a triacylglycerol was not published until 1992. In the crystal structure of 16.16.2 (9), the differences in chain lengths apparently force a 1,2 configuration. Chains 1 and 2, which are adjacent in a 1,2 configuration, form a triclinic ($T_{//}$) subcell instead of an $O_\perp$ subcell, but of the choices available the acetate group is thought to represent the effect of an acyl chain most reliably. Therefore, the conformation of the 16.16.2 molecule was chosen as starting conformation for the 10.12.10 molecule.

Shortening the chains in 16.16.2 to 10.12.2 automatically generates the shift of one methylene unit between two neighboring chains which is present in the C28 crystal structure (Fig. 5) and which is responsible for the 63° tilt. For p.p+2.p, this is not possible with the 1,3 configuration (Fig. 5). Lengthening the third "chain" from 2 to 10 C atoms can be done by simply adding a chain of 8 C atoms from the C28 structure, while preserving the bond and torsion angles with respect to the rest of the TAG molecule.

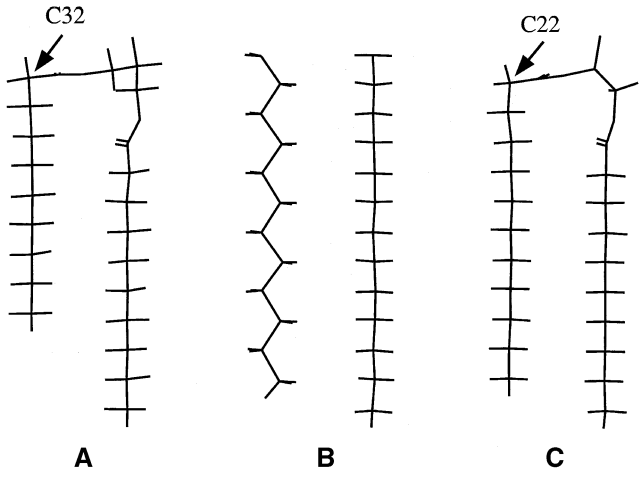

FIG. 5. Methylene shift between adjacent chains for the 1,2 and 1,3 configuration; the third chain is not shown. (A) 10.12.10 from 12.12.12 (1,3 configuration); (B) two adjacent chains from the C28 crystal structure; (C) 10.12.10 from 16.16.2 (1,2 configuration).

However, two problems remain. Firstly, chains 1 and 2, which are adjacent in a 1,2 configuration, form a $T_{//}$ subcell instead of an $O_{\perp}$ subcell. Secondly, the third "chain" in 16.16.2 is probably too short to truly represent a chain, which will have an influence on the conformation of this chain.

Hernqvist (18) dealt with the problem of the wrong subcell for β′-2 11.11.11 by combining a molecule of 12.12.12 with the $O_{\perp}$ subcell. However, his paper lacks a description of the procedure followed, the conformational changes involved are not discussed, final coordinates are not given, and no comparison with X-ray data is made. He extended his discussion to 16.18.16, a member of the p.p+2.p series (p even), but since the configuration of 16.18.16 was not clear, he used the 1,3 configuration, whereas according to Birker *et al.,* the 1,2 configuration should have been used. Hagemann and Rothfus (19) dealt with the problem of the wrong subcell for β′-2 10.10.10 by accepting the intramolecular $T_{//}$ subcell and forming dimers in such a way as to obtain an overall $O_{\perp}$ subcell. (That is, the acyl chain planes are parallel in pairs, but the acyl chain planes of two pairs are orthogonal. This is referred to as a hybrid subcell.) The same approach was used by Van Langevelde *et al.* (7), who showed that it is possible for β′-2 10.12.10 to obtain an overall $O_{\perp}$ subcell from an intramolecular $T_{//}$ subcell with one molecule in the asymmetric unit. Their molecules, however, are neither tilted nor bent.

We are not aware of any attempts to tackle the problem of the conformation of the third chain. We used the crystal structure of C28 to solve both problems simultaneously.

Three chains in the C28 crystal structure were considered to represent the three chains belonging to one TAG molecule. An initial model of a 10.12.10 molecule, generated from a 16.16.2 molecule as described above, was superimposed on the crystal structure of C28 as follows. Assuming the two neighboring chains from the C28 crystal structure were positioned as required by the β′ structure, these were overlaid with the two adjacent TAG chains. The third TAG chain was moved in plane with the third C28 chain by adjusting torsion angle H20-C20-C30-H30b (Fig. 6) from 173.2 to 180.0°. Two more torsion angles were adjusted to enlarge the bend angle, which was still too small. Torsion angle H30a-C30-O31-C31 was adjusted from −36.0 to −20.0° and torsion angle C30-O31-C31-O32 from 0.6 to 5.0°. The third C28 chain was shifted in the **b** and **c** direction until maximal overlap with the third chain from the TAG was reached (the **a** direction is constrained by the neighboring chains). The chains from the TAG were then discarded, leaving the glycerol moiety and the three C28 chains. The glycerol moiety and the three chains were connected, yielding a TAG molecule with the tilt and subcell required for the β′ structure.

Crystal building and energy minimization. The cell parameters for the structural model were taken from Birker *et al*., except for the angle β, which was taken to be 90°. This is justified by the pseudo-orthorhombicity following from the systematic absences in the diffraction data. *Ic*2*a* was chosen as the space group, which has the advantage over *I*2 of needing only one independent molecule in the unit cell instead of two,

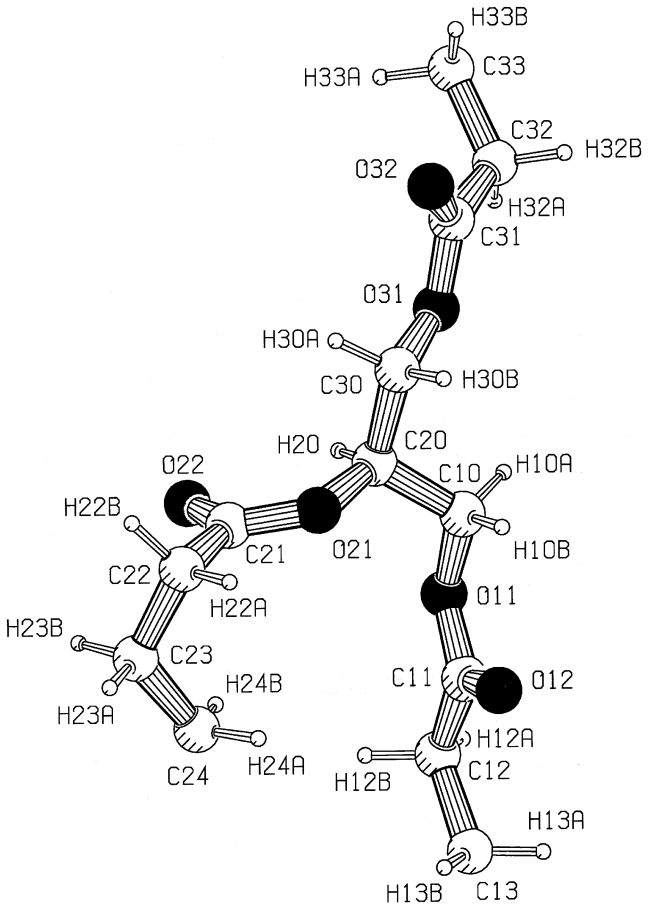

FIG. 6. Numbering of atoms for TAG molecules used in this paper. See Figure 1 for abbreviation.

decreasing the number of degrees of freedom. A TAG molecule in the conformation resulting from the procedure described in the previous section was placed in the unit cell as indicated by Birker *et al*. and space group symmetry was applied. The combination of unit cell, space group symmetry, and molecular shape imposed such strict conditions on the structure, that positioning the independent molecule to obtain reasonable packing was straightforward.

An energy minimization using the Dreiding 2.21 force field (20) was attempted. A straightforward calculation of atomic point charges from the quantum mechanical electrostatic potential would have been questionable, because of the uncertainty of the conformation. Based on the assumption that the bonded interactions together with the Van der Waals interactions would be sufficient to keep the structure together, no charges were initially used.

Given the uncertainties in both conformation and cell axes, it was decided to minimize the structure in a controlled way. First, only translations of the molecules, which were kept rigid, were allowed. Molecular rotations and unit-cell lengths were included successively. Next, four torsions connecting the third chain to the glycerol moiety (H20-C20-C30-O31, H30b-C30-O31-C31, C30-O31-C31-O32 and O31-C31-C32-

C33, see Fig. 6) were left flexible, but with fixed molecular orientations and unit-cell lengths. The resulting structure was considered to be sufficiently stable for a full minimization with fixed space-group symmetry. Since the structure minimized without any problems, the space-group constraint was lifted, leading to a readily minimized structure that remained of *Ic*2*a* symmetry. Note that the minimization algorithm includes second derivatives, ensuring the extrema to be minima. To explore the influence of crystal packing, a single molecule taken from the crystal structure was minimized *in vacuo*. The conformation remained stable.

Next, atomic point charges were calculated from the electrostatic potential from a single point self-consistent Field-Hartree Fock calculation with a 6-31G** basis set. As an additional constraint, the atomic point charges were restricted to reproduce the quantum mechanical molecular dipole. The structure was minimized fully (no constraints) with these point charges, using Ewald summation for both coulombic and Van der Waals interactions. Upon energy minimization without any constraints, the crystal structure remained orthorhombic, space group *Ic*2*a*, with $a = 22.83$ Å, $b = 5.56$ Å, $c = 60.23$ Å, $Z = 8$, $V = 7650$ Å^3, $\rho = 1.01$ g/cm^3.

Powder diffraction. Crystals of 10.12.10, with a melting point of 37.5°C, were grown from a melt on a sapphire plate to ensure thermal homogeneity. The plate was connected to a copper cell, which was kept at a constant temperature within 0.01°C during the growth process. Small plate-like crystals with an average aspect ratio of 1:10:100 along the **c**-, **a**-, and **b**-axes, respectively, were grown at 36.0°C. At 31.0°C, however, spherulites were obtained, which consisted of many very tiny (<1 μm) needle-shaped crystals. It is possible that the two crystal types grown at different temperatures were slightly different polymorphs (though both are β′), but any slight differences between the two crystal structures were not expected to be significant within our model.

The X-ray powder patterns were obtained using a Philips PW1710 (Almelo, The Netherlands) with Bragg–Brentano geometry and the crystals were put on a spinning sample holder. The radiation used was CuKα, the scan step size was 0.01° 2θ with a scan time of 1 s per step for $3.0° \leq 2\theta \leq 50.0°$.

DISCUSSION

Crystal building and energy minimization. The final model is shown in Figure 7; its coordinates and atomic charges can be obtained from the authors. In Table 2, the molecular mechanics' energies are given for three cases: for a molecule in its crystal environment, for the same molecule *in vacuo,* and for a molecule which was minimized *in vacuo*. Changing the molecular conformation to fit the crystal structure increased the energy by 4.71 kcal/mol, but the 140.0 kcal/mol decrease in energy resulting from Van der Waals and coulombic interactions in the crystal amply compensated for this slight gain in energy.

Chain packing and molecular conformation. The alkane chains of our β′-2 model packed in a $3 \times 1 \times 2$ supercell of the C28 structure, with one exception: the lower row of TAG molecules was turned by 180° around the **b**-axis. This means that the methyl group interactions no longer coincided with those of C28. If the methyl group interactions had been identical to those found in C28, one would have expected the twinning properties of the two structures to be the same. This was not the case. C28 readily twinned in the [001] direction, and the C28 structure was a polytypic modification of a monoclinic structure, with $\alpha = 91.67°$. 12.14.12 readily twinned in the [001] direction, but (in the same cell setting) the angle β alternated between 89 and 91°. These were the same twinning angles found for a polymorph of C33 (88.8 and 91.2°), both in magnitude and direction (21). In this structure, however, the chains, though forming an $O_\perp$ subcell, were not tilted.

This leaves room for speculations on the exact methyl group interactions, but the experimental data are not good enough to decide on this subtlety: Calculated powder diagrams of the true $3 \times 1 \times 2$ supercell of the C28 structure and of a structure in which the first two rows of chains adjacent in the **c**-direction are turned by 180° around the **b**-axis are the same within experimental error. The effects on the methyl group interactions will be negligible for the calculation of powder diagrams and molecular mechanics' energies. This is especially true for nonacademic cases, such as margarines and cocoa butter, which are mixtures of TAG with and without double bonds, where β′ is a metastable modification.

The subcell of our model differs from those published before. This concerns the presence of an intramolecular $O_\perp$ subcell, not just an overall $O_\perp$ subcell. Changing the intramolecular $T_{//}$ subcell into an $O_\perp$ subcell appeared to be easiest when done by leaving the first chain unchanged and replacing the second by a chain from the C28 crystal structure as described above. The net effect is a turn around the C21-C22 bond by 60° (Fig. 8). This should not lead to any significant gain or loss in energy, as the two conformations at C22 are more or less mirror images. The same will hold for a 1,3 configuration of the TAG, since the differences between the two con-

TABLE 2
Molecular Mechanics' Energies for a Molecule of the Final Structure

	Bonded interactions (kcal/mol)	Nonbonded interactions (kcal/mol)	Total (kcal/mol)
In crystal	17.86	–139.0	–121.2
From crystal *in vacuo*	17.86	0.9331	18.79
Minimized *in vacuo*	15.73	–1.643	14.08

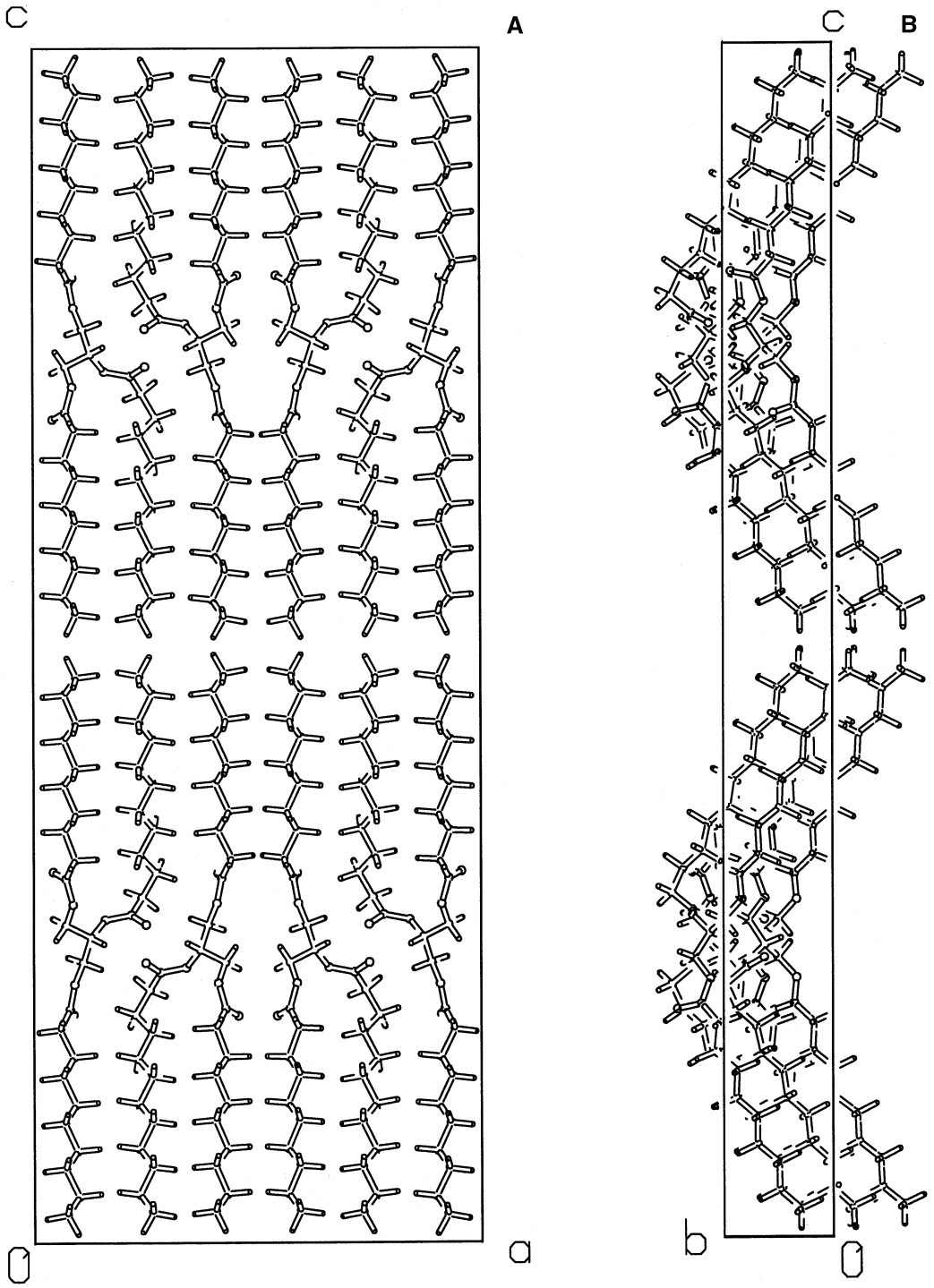

FIG. 7. (A) The final model for 10.12.10 β′-2 viewed along the **b**-axis. (B) Final model for 10.12.10 β′-2 viewed along the **a**-axis.

figurations are negligible in this region of the TAG. As mentioned above, introducing the 1,2 configuration for p.p+2.p automatically generates the methylene shift between two neighboring chains needed for the C28 structure and responsible for the 63° tilt, which is not possible with the 1,3 configuration. The bend in the molecule also follows directly from the 1,2 configuration, whereas the 1,3 configuration yields a straight molecule. The 1,2 configuration and the conformation of chains 1 and 2 in this β′ structure are therefore very plausible. We do not claim, however, that our intramolecular $O_{\perp}$ subcell is necessarily the only possibility.

The conformation of the third chain is less certain and may contain one or more incorrect torsion angles. As expected, chain 3 changed the most during energy minimization. Tor-

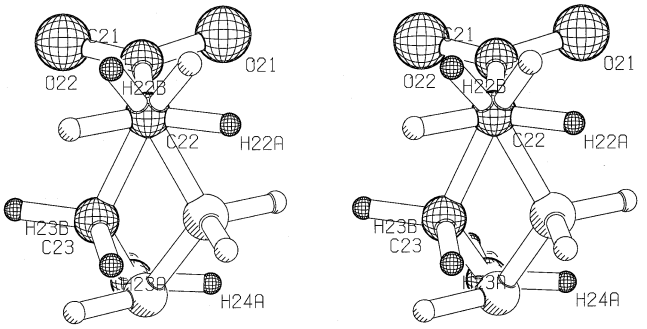

FIG. 8. Stereoplot of the two superimposed conformations at C22. The ester fragments (O21-C21-O22) and C22 overlap. The first chain (not shown) forms an intramolecular $T_{//}$ subcell with the $-CH_2-$ units in their original position (shown shaded) and an intramolecular $O_{\perp}$ subcell with the $-CH_2-$ units in their new position (shown with a net-like pattern). See Figure 3 for abbreviations.

sion angle H30a-C30-O31-C31, in particular, changed from −36.0 to 51.3°, bending away the carbonyl group ≈90° compared to its starting position in the conformation from the 16.16.2 crystal structure. The resulting conformation is slightly more favorable energetically and a conformational analysis of this torsion angle shows that the energy of the 10.12.10 molecule lies within a 4.5 kcal/mol window for the complete range −50° < H30a-C30-O31-C31 < 150°, so the new conformation is acceptable.

Powder diffraction. In Figure 9, the powder pattern calculated for our model structure is compared with the experimental powder diagram of the β′ crystals grown at 31.0°C. Some experimental information was imposed to emphasize the differences caused by the contents of the unit cell. The unit cell parameters were set to their experimental values and the zero point was set to 0.2° 2θ. Some preferred orientation was taken

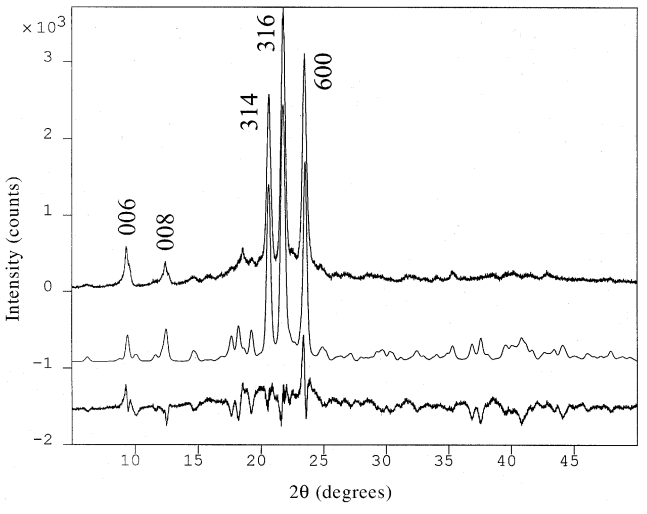

FIG. 9. Experimental (top), calculated (middle), and difference (bottom) powder diagrams. The cell parameters of the final model were set to their experimental values and some preferred orientation was included, as well as the zero point error. The experimental powder diagram was obtained from the crystals grown at 31.0°C.

into account using the March–Dollase distribution function with direction [001] (see below) and $G_1 = 0.8$. The intensity of the 002 peak is decreased by the diaphragm and can only be used for qualitative purposes. It is therefore not included in our comparisons, but the calculated 002 peak has a much higher intensity than measured, as was expected.

Neglecting the glycerol groups, the pseudoperiodicity in the **a** direction should be one third of the **a**-axis. However, according to Birker *et al.*, "all reflections $h = 3n$ would then be very weak. The diffraction patterns . . . show that this is not the case," and they therefore rejected the presence of a true $O_{\perp}$ subcell. We disagree on this point. With pseudo threefold periodicity, the $h \neq 3n$ reflections should be very weak, as found in the experimental pattern. Note that the $O_{\perp}$ subcell itself has a two-dimensional "subcell" with respect to projection on the **ac**-plane. Due to the inclination of the chains, only a one-dimensional "subcell" with respect to projection on the **a**-axis survives for the overall structure. So among the *h*00 reflections, the 300 reflection should be weak and the 600 reflection should be strong. This too is confirmed by the experimental data. Additional evidence for an $O_{\perp}$ subcell comes from atomic force microscopy measurements on the (001) plane of 12.14.12, which confirm the methyl groups are positioned as needed for an $O_{\perp}$ subcell tilted by 65° (22).

We expect the powder diagram from the polymorph grown at 36.0°C to suffer from preferred orientation. The plate-like crystals will lie parallel to the sample holder, biasing the orientational distribution. In the Bragg–Brentano geometry used, this means that reflections from planes more or less parallel to the (001) plane will be more pronounced than those more or less parallel to the (100) and (010) planes. Since the relative intensities of the 00*l* reflections will be unaffected (these are reflections onto the same set of Miller planes which have identical orientations), we can use the preferred orientation to reliably compare the calculated and measured 00*l* reflections. The intensities of the other reflections will be unreliable and should not be used to check the model.

In Figure 10, the calculated 00*l* reflections are compared with the experimental powder diagram of the β′ grown at 36.0°C. The 002 reflection (not shown) is again calculated to be much stronger than measured; the 0,0,14 reflection overlaps with the 316 reflection and cannot be compared. Up to 0,0,24, the orders of magnitude are correct. Contrary to the short-spacing reflections, which are completely dictated by the chains, the 00*l* reflections are sensitive to the positions of the atoms of the glycerol group (especially the oxygen atoms). Since this is also the most flexible and least certain part of the structure, they will be mainly responsible for the differences between the experimental and the calculated powder diagram. After submitting our paper, additional experimental evidence was published (7), which is the subject of a separate publication (23).

Extension to other β′ structures. As mentioned above, there are several β′ structures depending on p, q, and r and the introduction of double bonds. The following similarities and dissimilarities of our structure with respect to other β′ structures can be noted.

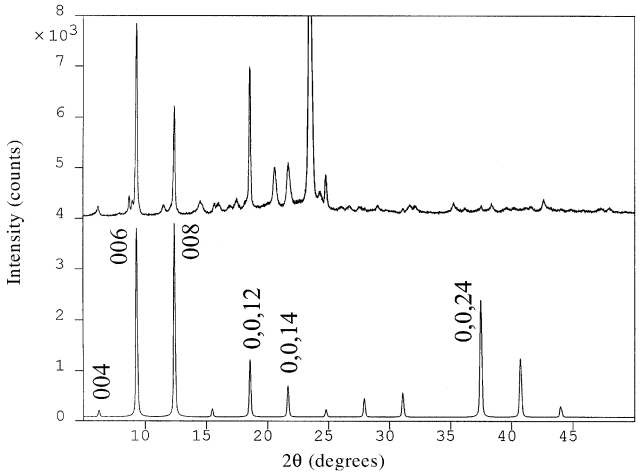

FIG. 10. Experimental (top) vs. calculated (bottom) powder diagram. The cell parameters of the models, as well as the zero point error, were set to their experimental values; the experimental powder diagram was obtained from the crystals grown at 36.0°C.

The extension of the 10.12.10 structure to the other members of the p.p+2.p series is straightforward, and the unit cells and atomic coordinates for all members can be calculated using the method published for *n*-alkanes (24).

One of the most important fatty acids in nature is oleic acid (*cis*-9-octadecenoic acid), which contains a *cis* double bond. The structure of petroselinic acid (*cis*-6-octadecenoic acid) (25) shows that this does not *a priori* rule out the structural features presented in this paper: the methyl-terminated part of the chains in the crystal coincide with those in C28, reproducing the $O_{\perp}$ subcell and the 65° tilt, as the authors themselves point out. The *cis* double bond disrupts this pattern, but only to continue it on its other side. This would pave the way for modeling the β′ structure of 16.18:1.16 and 18.18:1.18 (usually called POP and SOS, respectively, after the initials of the trivial names of the corresponding fatty acids, i.e., palmitic, oleic, and stearic acids). The double bond in petroselinic acid is shifted by three carbon atoms with respect to the double bond in oleic acid. This is a serious drawback, since it changes the parity of the methyl-terminated alkane part of the acid, and from *n*-alkanes this change in parity is known to have a profound effect on the polymorph found. Note that POP and SOS will probably have a 1,3 configuration and pack together in a β′-3 arrangement in order to avoid mixing of saturated and unsaturated chains.

The unit cell of the tilted β′ structure of 12.12.12 (a member of the p.p.p series, p even) shows the same *a*, *b*, α, β, and γ as β′-2 p.p+2.p, suggesting an $O_{\perp}$ subcell with chains tilted at 63° (26). The authors mention an angle of tilt of 62°. β′ p.p.p probably has a 1,3 configuration, but this has no consequences for the conformation at C22 other than its label; it is now C32 (Fig. 5). Twisting the third chain from an intramolecular $T_{//}$ subcell to an intramolecular $O_{\perp}$ subcell at C32 by means of two simultaneous 60° rotations around the C31-C32 and C32-C33 bonds provides a comfortable transition pathway for the rapid β′-2 → β-2 phase transition observed (≈1 min), with hardly noticeable changes in the overall conformation. If the bend in the p.p+2.p β′-2 molecule was a consequence of its 1,2 configuration, a p.p.p β′-2 molecule is not expected to be bent, just tilted (like the molecules in C28 itself).

The structure of β′-2 11.11.11 (a member of the p.p.p series, p odd) proposed by Hernqvist (18) fits in seamlessly. The cell parameters *b*, α, β, and γ are again equal to those of β′-2 10.12.10; *a* is slightly larger: 23.6 Å instead of 22.9 Å. Starting with a molecule of 12.12.12, the intramolecular $O_{\perp}$ subcell can be introduced as described in the present paper, followed by shortening to 11.11.11.

ACKNOWLEDGMENTS

We thank Arjen J. van Langevelde, Kees F. van Malssen, René Peschar, and Henk Schenk for stimulating discussions, and Hugo Meekes, Piet Bennema, and Elias Vlieg for helpful comments and critical reading of the manuscript. The authors wish to express their appreciation to Eckhard Flöter (Unilever Research Laboratorium, Vlaardingen) for providing 10.12.10, to Enno A. Klop (Akzo Nobel Central Research, Arnhem) for additional diffraction measurements, and to Jan H. Noordik (CAOS/CAMM Center) for overall project coordination. The investigations were supported by the Netherlands Organization for Chemical Research (NWO-CW) within the framework of the PPM/CMS Crystallization project.

REFERENCES

1. De Jong, S., Ph.D. Thesis, University of Utrecht, The Netherlands, 1980, p. 5.
2. Larsson, K., The Crystal Structure of the β-Form of Trilaurin, *Ark. Kemi 23*:1–15 (1965).
3. Jensen, L.H., and A.J. Mabis, Refinement of the Structure of β-Tricaprin, *Acta Crystallogr. 21*:770–781 (1966).
4. Gibon, V., P. Blanpain, B. Norberg, and F. Durant, New Data about Molecular Structure of β-Trilaurin, *Bull. Soc. Chim. Belg. 93*:27–34 (1984).
5. Van Langevelde, A., K. van Malssen, F. Hollander, R. Peschar, and H. Schenk, Structure of Mono-Acid Even-Numbered β-Triacylglycerols, *Acta Crystallogr. B55*:114–122 (1999).
6. Birker, P.J.M.W.L., S. de Jong, E.C. Roijers, and T.C. van Soest, Structural Investigations of β′ Triacylglycerols: An X-Ray Diffraction and Microscopic Study of Twinned β′ Crystals, *J. Am. Oil Chem. Soc. 68*:895–906 (1991).
7. Van Langevelde, A., K. van Malssen, E. Sonneveld, R. Peschar, and H. Schenk, Crystal Packing of a Homologous Series β′-Stable Triacylglycerols, *Ibid. 76,* 603–609 (1999).
8. Boistelle, R., B. Simon, and G. Pèpe, Polytypic Structures of *n*-$C_{28}H_{58}$ (octacosane) and *n*-$C_{36}H_{74}$ (hexatriacontane), *Acta Crystallogr. B32*:1240–1243 (1976).
9. Goto, M., D.R. Kodali, D.M. Small, K. Honda, K. Kozawa, and T. Uchida, Single Crystal Structure of a Mixed-Chain Triacylglycerol: 1,2-Dipalmitoyl-3-acetyl-*sn*-glycerol, *Proc. Nat. Acad. Sci. USA 89*:8083–8086 (1992).
10. *Cerius*^{2} *User Guide,* Version 3.5, Molecular Simulations Inc., San Diego, 1998.
11. Allen, F.H., and O. Kennard, 3D Search and Research Using the Cambridge Structural Database, *Chem. Design Autom. News 8*:1,31–337 (1993).
12. Pascher, I., S. Sundell, and H. Hauser, Glycerol Conformation and Molecular Packing of Membrane Lipids. The Crystal Structure of 2,3-Dilauroyl-D-glycerol, *J. Mol. Biol. 153*:791–806 (1981).

13. Dorset, D.L., and W.A. Pangborn, Polymorphic Forms of 1,2-Dipalmitoyl-*sn*-glycerol: A Combined X-ray and Electron Diffraction Study, *Chem. Phys. Lipids 48*:19–28 (1988).
14. Harlos, K., H. Eibl, I. Pascher, and S. Sundell, Conformation and Packing Properties of Phosphatidic Acid: The Crystal Structure of Monosodium Dimyristoylphosphatidate, *Ibid. 34*: 115–126 (1984).
15. Hitchcock, P.B., R. Mason, K.M. Thomas, and G.G. Shipley, Structural Chemistry of 1,2 Dilauroyl-DL-phosphatidylethanolamine: Molecular Conformation and Intermolecular Packing of Phospholipids, *Proc. Nat. Acad. Sci. USA 71*:3036–3040 (1974).
16. Pascher, I., and S. Sundell, Membrane Lipids: Preferred Conformational States and Their Interplay. The Crystal Structure of Dilauroylphosphatidyl-*N*,*N*-dimethylethanolamine, *Biochim. Biophys. Acta 855*:68–78 (1986).
17. Pearson, R.H., and I. Pascher, The Molecular Structure of Lecithin Dihydrate, *Nature 281*:499–501 (1979).
18. Hernqvist, L., On the Crystal Structure of the β'_1-Form of Triglycerides and the Mechanism Behind the $\beta'_1 \rightarrow \beta$ Transition of Fats, *Fat Sci. Technol. 90*:451–454 (1988).
19. Hagemann, J.W., and J.A. Rothfus, Effects of Chain Length, Conformation and α-Form Packing Arrangement on Theoretical Monoacid Triglyceride β′-Forms, *J. Am. Oil Chem. Soc. 65*:638–646 (1988).
20. Mayo, S.L., B.D. Olafson, and W.A. Goddard III, DREIDING: A Generic Force Field for Molecular Simulations, *J. Phys. Chem. 94*:8897–8909 (1990).
21. Piesczek, W., G.R. Strobl, and K. Malzahn, Packing of Paraffin Chains in the Four Stable Modifications of *n*-Tritriacontane, *Acta Crystallogr. B30*:1278–1288 (1974).
22. Birker, P.J.M.W.L., and J.C.G. Blonk, Alkyl Chain Packing in a β′ Triacylglycerol Measured by Atomic Force Microscopy, *J. Am. Oil Chem. Soc. 70*:319–321 (1993).
23. Van de Streek, J., P. Verwer, R. de Grelder, and F. Hollander, New Evidence for β′ p.p+2.p Triacylglycerol Crystal Structure, *Ibid. 77,* in press.
24. Nyburg, S.C., and J.A. Potworowski, Prediction of Units Cells and Atomic Coordinates for the *n*-Alkanes, *Acta Crystallogr. B29*:347–352 (1973).
25. Kaneko, F., M. Kobayashi, Y. Kitagawa, Y. Matsuura, K. Sato, and M. Suzuki, Structure of the Low-Melting Phase of Petroselinic Acid, *Acta Crystallogr. C48*:1054–1057 (1992).
26. Buchheim, W., and E. Knoop, Elektronenbeugungs-Untersuchung von Trilaurin, *Naturwissenschaften 56*:560–561 (1969).
27. Spek, A.L., PLATON, an Integrated Tool for the Analysis of the Results of a Single Crystal Structure Determination, *Acta Crystallogr. A46*:C-34 (1990).

[Received December 15, 1998; accepted June 16, 1999]